Reflection of metastable argon atoms from an evanescent wave

W. Seifert, C. S. Adams, V. I. Balykin, C. Heine,* Yu. Ovchinnikov,† and J. Mlynek

Fakultät für Physik, Universität Konstanz, 78434 Konstanz, Germany

(Received 23 September 1993)

The reflection of metastable argon atoms from evanescent waves produced by total internal reflection and surface-plasmon excitation is investigated. We study the departure from ideal specular reflection by comparing our experimental results with a Monte Carlo simulation of the reflection process. The observed broadening of the reflection beam was found to be caused predominantly by fluctuations of the dipole force. We show that the surface plasmon produces significant enhancement of the evanescent-wave intensity without degrading the quality of reflection. In addition, the number of spontaneous emissions occurring during the reflection process was investigated by comparing the reflectivity of evanescent-wave mirrors based on open and closed transitions in argon. An open-transition mirror selectively reflects atoms which do not undergo spontaneous emission. For a large detuning, the average number of spontaneous emissions for reflected atoms was < 0.11.

I. INTRODUCTION

In 1929 Stern and colleagues marked the beginnings of atom optics by demonstrating the reflection and diffraction of atoms from metallic and crystalline surfaces [1]. In recent years there has been an explosion of interest in this field stimulated, in part, by the rapid progress in techniques to manipulate the trajectories of neutral atoms using light forces [2]. Of considerable interest is the development of mirrors for atoms. An atom mirror could be used for the storage of atoms in a cavity, as a component in an atom interferometer, or, using a concave mirror, for focusing of atomic beams. There are two approaches to realize atom mirrors; reflection from surfaces, first demonstrated almost 70 years ago and now developed into a useful tool in surface science [3], or using potentials induced by static or optical electromagnetic fields.

This paper considers reflection of atoms by a light-induced potential. In 1982 Cook and Hill [4] suggested that a near-resonant evanescent light wave could be used to reflect atoms. An evanescent wave is produced by total internal reflection of a light beam at the interface between a dielectric and the vacuum. The light intensity decays exponentially with distance from the surface. If the light field is blue detuned from the atomic resonance, an incident atomic beam experiences a repulsive potential with an approximately exponential dependence. Reflection of atoms from an evanescent wave was first observed by Balykin et al. [5]. In this experiment sodium atoms were reflected up to a maximum angle of 0.4°. At small incident angles, the reflectivity of the mirror was shown

to be close to 100%. In another experiment Kasevich et al. [6] demonstrated reflection under normal incidence by dropping a cloud of cold atoms above an evanescent wave. Two bounces of the reflected atoms were observed. More recently, by using a concave mirror to confine the horizontal motion, a group at Ecole Normale Supérieure, Paris, has observed up to ten bounces [7].

The use of evanescent fields as an atom mirror has a number of advantages over direct reflection from a surface: The evanescent-wave potential (assuming adiabatic evolution and no spontaneous emission) is purely repulsive, whereas atom-surface potentials contain an attractive term due to the van der Waals force, which leads to large sticking probabilities. Evanescent-wave reflection places less stringent demands on the surface quality. Also evanescent waves may be used to reflect atoms in internal states other than the ground state, for example, metastable rare gas atoms.

For an evanescent-wave mirror, intense light fields are required for two reasons, first to permit the reflection of more energetic atoms, and second the threat of spontaneous emission may be reduced without compromising the optical potential by increasing the intensity together with the laser detuning. As limited laser power is available, techniques to enhance the evanescent field are attractive. Recently reflection of rubidium [8] and neon [9] by a surface-plasmon-enhanced evanescent wave have been demonstrated. In both experiments significant broadening of the reflected beam was observed, but possible mechanisms for the additional divergence were not investigated. Another promising enhancement technique for atom-mirror applications uses stratified dielectric media [10].

In this paper we present a detailed study of the reflection of metastable argon atoms from a near-resonant evanescent wave. Reflection by evanescent waves produced by total internal reflection and surface-plasmon excitation are compared. Reflection of metastable argon atoms from an evanescent wave enhanced by a stratified

---

layer is reported elsewhere [11]. Many applications of atom mirrors require near-perfect reflection. Although reflection of atoms by evanescent wave has been demonstrated by a number of authors, little is known about the quality of the reflection process. By comparing our experimental results with Monte Carlo simulations, we are able to assess the relative importance of different mechanisms which lead to a departure from ideal specular reflection. In particular, the effects of fluctuations in the dipole force and the Gaussian laser beam profile are investigated. In addition, we study the number of spontaneous emissions occurring during the reflection process by comparing the reflectivity of evanescent-wave mirrors using "open" and "closed" transitions in argon. By comparing the number of reflected atoms, one can estimate the average number of spontaneous emissions.

The paper is organized as follows. In Sec. II we present a brief introduction to the reflection of atoms from an evanescent wave. The conditions for specular reflection are considered and the properties of evanescent waves produced by total internal reflection and by surface-plasmon excitation are discussed. In Sec. III the experimental setup is described. In Sec. IV the experimental results are presented and compared to the predictions of a Monte Carlo simulation of the reflection process. The article concludes with a summary and outlook in Sec. V.

II. REFLECTION OF ATOMS FROM AN EVANESCENT WAVE

The reflection of atoms from an evanescent wave is depicted schematically in Fig. 1. If a Gaussian beam is totally internally reflected at a dielectric-vacuum interface, the electric field in the vacuum is

$$E(x, y, z) = E_0 \exp\left[-\alpha z - \left(\frac{x}{w_x}\right)^2 - \left(\frac{y}{w_y}\right)^2 \right]$$
$$\times \exp(ik_x x) , \qquad (2.1)$$

where x and z are the coordinates parallel and perpendicular to the interface, E_0 is the maximum electric field amplitude (see below), k_x is the k vector parallel to the interface, and $w_{x,y}$ are the Gaussian beam waists in the x, y directions. The evanescent wave propagates parallel to the interface with wave vector

$$k_x = \frac{2\pi}{\lambda} n \sin\theta_i \qquad (2.2)$$

and decays exponentially away from the surface with characteristic length $1/\alpha$, where

$$\alpha = \frac{2\pi}{\lambda}(n^2 \sin^2\theta_i - 1)^{1/2} , \qquad (2.3)$$

and θ_i is the angle of incidence of the laser beam.

The Rabi frequency $\omega_1(\mathbf{r})$ is proportional to the electric field amplitude, therefore

$$\omega_1(\mathbf{r}) = \omega_{1,\text{max}} \exp\left[-\alpha z - \left(\frac{x}{w_x}\right)^2 - \left(\frac{y}{w_y}\right)^2 \right] . \quad (2.4)$$
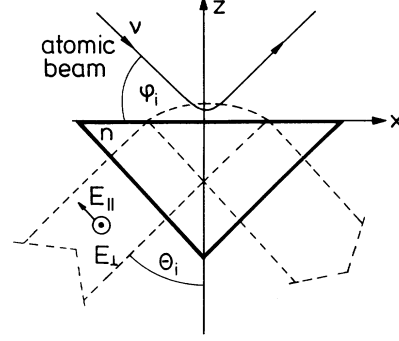
The light force experienced by an atom in the evanes-

FIG. 1. Schematic representation of reflection of an atomic beam from an evanescent wave. The atomic beam is incident at an angle φ_i relative to the surface plane. The laser beam is incident at an angle θ_i relative to the surface normal.

cent wave is conveniently divided into the spontaneous force and the dipole force [13]: The spontaneous force acts parallel to the surface and is given by

$$\mathbf{F}_{\text{spont}} = \hbar k_x \frac{\Gamma}{2} \mathbf{e}_x \qquad (2.5)$$

for a large laser power, where Γ is the spontaneous decay rate of the excited state. The dipole force has components parallel and perpendicular to the surface,

$$\mathbf{F}_{\text{dip}\parallel} = -\frac{\hbar\omega_1^2}{\Omega} \left(\frac{x}{w_x^2}\mathbf{e}_x + \frac{y}{w_y^2}\mathbf{e}_y \right) ,$$
$$(2.6)$$
$$\mathbf{F}_{\text{dip}\perp} = -\alpha\frac{\hbar\omega_1^2}{2\Omega}\mathbf{e}_z ,$$

where $\Omega = \sqrt{\Delta^2 + \omega_1^2}$ is the effective Rabi frequency, $\Delta = \omega_L - \omega_0 - k_x v$ is the atom-laser detuning including the Doppler shift, and v is the atomic velocity.

Both the spontaneous force and the tangential components of the dipole force lead to nonspecular reflection. For an atom mirror, large laser intensities are required, therefore $\omega_1 \gg \Gamma$ and the spontaneous force is negligible. However, spontaneous emission also induces fluctuations in the sign of the dipole force which also results in nonspecular reflection. The effect of spontaneous emission will be discussed in detail in Sec. IV C.

For specular reflection, one requires that the average number of spontaneous emissions during the reflection process is small and that $F_{\text{dip}_z} \gg F_{\text{dip}_{x,y}}$. The tangential components of the dipole force F_{dip_x} and F_{dip_y} arise due to the finite size of the laser beam. Their effect is equivalent to a diverging lens. The focal length can be estimated from the effective radius of curvature of the evanescent field. In the plane containing the x axis, the radius of the $1/e$ contour is $R = \frac{1}{2}(\alpha w_x^2 + 1/\alpha)$. The focal length for normal incidence is $R/2$, therefore in the x-z plane

$$f_x \sim \frac{\alpha w_x^2}{4}. \qquad (2.7)$$

As $1/\alpha < \lambda$, it follows that $\alpha \gg \frac{1}{w_x} + \frac{1}{w_y}$, $F_{\text{dip}_z} \gg$

$F_{\mathrm{dip}_{x,y}}$, and therefore the defocusing effect is relatively small. For glancing incidence the effective focal length is larger, but astigmatic aberrations become important. A more accurate determination of these effects is provided by the Monte Carlo simulation presented in Sec. IV C.

The evanescent wave is governed by two free parameters: the angle of incidence of the light beam θ_i and the refractive index of the dielectric n. For an atom mirror, a short decay length is desirable in order to reduce the effective light-atom interaction time and hence the probability of spontaneous emission. Thus it is preferable to use a dielectric medium with a high refractive index and an incidence angle well away from the critical angle.

A. Simple evanescent wave

For total internal reflection at a dielectric-vacuum interface, the amplitude of the evanescent wave [E_0 in Eq. (2.1)] is related to the amplitude of the incident laser field in the dielectric E_d by

$$| E_o |^2 = \beta_{\|,\perp}^2 | E_d |^2, \tag{2.8}$$

where $\beta_{\|,\perp}$ are the Fresnel coefficients for light polarized parallel (TM) and perpendicular (TE) to the plane of incidence [14]:

$$\beta_\|^2 = 4n^2 \cos^2 \theta_i / (\cos^2 \theta_i + n^4 \sin^2 \theta_i - n^2) \tag{2.9}$$

and

$$\beta_\perp^2 = 4n^2 \cos^2 \theta_i / (n^2 - 1). \tag{2.10}$$

For a fused silica prism $n = 1.45$ and an incidence angle $\theta_i = 45°$, $\beta_\|^2 = 6.9$ and $\beta_\perp^2 = 3.8$, whereas for $\theta_i = 60°$, $\beta_\|^2 = 1.4$ and $\beta_\perp^2 = 1.9$. Thus the optimum polarization of the incoming light beam depends on the refractive index and the angle of incidence.

B. Surface-plasmon-enhanced evanescent wave

Surface plasmons are charge density waves that propagate along a metal-dielectric interface [15]. The k-vector component along x for a surface plasmon is

$$k_x = \frac{\omega}{c} \sqrt{\frac{\varepsilon_1'}{\varepsilon_1' + 1}}, \tag{2.11}$$

where $\varepsilon_1 = \varepsilon_1' + i\varepsilon_1''$ is the relative permittivity of the metal. A surface plasmon can be excited by a TM polarized evanescent wave propagating along the metal-dielectric interface. If the k vector of the evanescent wave matches that of the surface plasmon there is a resonant coupling into the plasmon mode. The resonance condition, given by equating (2.2) and (2.11), defines the optimum angle of incidence of the laser beam,

$$\sin^2 \theta_{i,\mathrm{opt}} = \frac{\varepsilon_1'}{\varepsilon_2(\varepsilon_1' + 1)}, \tag{2.12}$$

where ε_2 is the relative permittivity of the dielectric. For a glass substrate ($n = \sqrt{\varepsilon_2} = 1.45$) with a silver film ($\varepsilon_1' \sim -30$), $\sin \theta_{i,\mathrm{opt}} = 44.6°$. The decay length of the surface-plasmon evanescent wave is given by (2.3) and (2.12),

$$\alpha = \frac{2\pi}{\lambda} \sqrt{\frac{-1}{\varepsilon_1' + 1}}. \tag{2.13}$$

An attractive feature of a plasmon wave is the large field enhancement of the initial laser beam intensity. The field enhancement γ^2, defined as the ratio between the maximum intensity of the evanescent field with and without plasmon excitation assuming ideal coupling, is

$$\gamma^2 = \frac{\varepsilon_1'^2}{2\varepsilon_2\varepsilon_1''} \frac{\sqrt{-\varepsilon_1'(\varepsilon_2 - 1) - \varepsilon_2}}{1 - \varepsilon_1'}. \tag{2.14}$$

For a solution $\varepsilon_1' < 0$ and $\varepsilon_2 < | \varepsilon_1' |$ are required, which is true for most metal-dielectric interfaces. As an example, consider a quartz dielectric with a silver layer. The maximum field enhancement γ^2 depends critically on the values for ε_1' and ε_1''. At $\lambda = 800$ nm the maximum enhancement γ^2 is between 15 and 100 [16,17] depending on the reference for ε_1' and ε_1''. In practice, the enhancement is limited by imperfections in the silver film which increase the radiation damping.

C. Atom-surface interaction

When an atom approaches a conducting wall, its energy levels are shifted for two reasons: First, the wall changes the vacuum field distribution and its fluctuations. Second, the atom reacts on its own field reflected from the conducting surface [18].

If the atom-surface separation is smaller than the wavelengths of the atomic transitions divided by 2π, the atomic levels are shifted by the van der Waals energy ΔE_{VW}

$$\Delta E_{\mathrm{VW}} = -\frac{1}{4\pi\varepsilon_0} \frac{1}{16z^3} (d_\rho^2 + 2d_z^2), \tag{2.15}$$

where d_ρ and d_z are the components of the electric dipole moment parallel and perpendicular to the wall. As the atom-surface separation increases, the van der Waals energy changes to the Casimir-Polder energy ΔE_{CP},

$$\Delta E_{\mathrm{CP}} = -\frac{1}{4\pi\varepsilon_0} \frac{3\hbar c}{8\pi z^4} \alpha_0, \tag{2.16}$$

where α_0 is the static electric polarizability.

An exited state experiences an additonal energy shift ΔE_{exc} that oscillates with an amplitude which is for small separations of the order of Planck's constant $\hbar$ times the line width Γ of the transition and is for large separations and a dipole moment parallel to the surface inversely proportional to the atom wall separation.

All these level shifts alter the atom-mirror potential and apply a force to the atom as they depend on the atom-surface separation. In addition they modify the detuning of the evanescent wave, because they change the

atomic transition frequency when the atom approaches the surface. They become significant at separations smaller than 50 nm.

If the conducting plane is replaced by a nondispersive dielectric boundary with permittivity ε, these energy shifts are reduced by $\frac{\varepsilon - 1}{\varepsilon + 1}$.

III. EXPERIMENT

The experimental setup is shown in Fig. 2. The atomic beam was produced by a supersonic expansion of argon at room temperature. The argon atoms are excited into the metastable state $1s_5$ by electron bombardment. The atomic beam had an average longitudinal velocity of 560 ms^{-1} and a relative velocity spread $v/\Delta v \sim 10$. The atomic beam was collimated by two slits (S_1 and S_2 in Fig. 2): S_1 was 100 μm wide and 8 mm high, S_2 was 10 μm wide and 3 mm high and placed 0.95 m downstream. The resulting angular divergence of the atomic beam was 0.1 mrad.

The simple evanescent wave was produced by total internal reflection of a laser beam within a glass prism with refractive index $n = 1.45$. The laser beam was incident at $\theta_i = 45°$ and polarized (E-field direction) parallel to the plane of incidence (TM polarization) to maximize the enhancement factor (see Sec. II). The decay length of the evanescent field (2.3) was $1/\alpha = 550$ nm. The prism had a surface quality of $\lambda/20$.

For the plasmon experiments, a surface plasmon was excited by a TM polarized laser beam incident on a 52 nm thick silver layer evaporated on a glass prism ($n = 1.45$). The angle of incidence was optimized ($\theta_i = 44.6°$) by minimizing the reflected laser intensity. The decay length of the evanescent field (2.13) was $1/\alpha = 640$ nm. The similarity in the decay length simplifies direct comparison of the experimental results.

Reflection of atoms from evanescent light fields resonant with both the $1s_5$-$2p_9$ transition ($\lambda = 811.8$ nm) and the transition $1s_5$-$2p_8$ ($\lambda = 801.7$ nm) was investigated (see argon term scheme in Fig. 2). The light was produced by a single mode Ti:sapphire ring laser (Coherent 899-21) with a maximum power of 3 W. The laser was actively stabilized by locking to a temperature stabilized reference cavity. The cavity could be tuned electronically. The detuning was calibrated using an optical spectrum analyzer and an electro-optic modulator to produce sidebands at a known frequency. The laser beam was focused using cylindrical optics to produce an elliptical waist on the surface of the prism. For the normal and plasmon-enhanced evanescent waves, the dimensions of the waist were $w_x = 10.5$ mm, $w_y = 0.4$ mm and $w_x = 12.0$ mm, $w_y = 0.7$ mm, respectively.

The position and zero angle of the prism relative to the atomic beam were adjusted by monitoring the atomic intensity on axis. The angle of incidence φ_i was adjusted by tilting the prism. The relative angle could be controlled with an accuracy of 0.1 mrad. The component of the atomic beam which completely missed the prism defines the zero position in the detector plane. The atomic beam was detected by a channeltron with a 50 μm entrance slit (S_3) placed 0.58 m downstream of the interaction region. The spatial distribution of the reflected atoms was recorded by scanning the detector and slit assembly in the transverse direction. The channeltron is insensitive to atoms which have decayed to the electronic ground state.

IV. RESULTS AND DISCUSSION

A. Reflection by a simple evanescent wave

A preliminary measurement was made to test for reflection of metastable atoms directly from the glass surface. No reflected peak was observed. This result agrees with previous work on the reflection of metastable atoms from surfaces where survival probability for glancing angle reflection of order 10^{-4} has been reported [19].

When an evanescent light field resonant with the "closed" transition ($1s_5$-$2p_9$, $\lambda = 811.8$ nm) was produced at the prism surface, a reflected atomic beam could be clearly resolved. Figure 3 shows the distribution of reflected atoms for a range of incident angles. The incident laser power was 1 W, corresponding to a maximum Rabi frequency $\omega_{1,\text{max}} = 2\pi \times 770$ MHz. The laser was blue detuned by $\Delta = \omega_L - \omega_0 = 2\pi \times 900$ MHz. The atomic and laser beams copropagated, therefore the effective detuning in the moving frame of the atom was $\Delta = 2\pi \times 200$ MHz. In Fig. 3, the peak at $\varphi_i = 0$ mrad corresponds to atoms which missed the prism and traveled straight to the detector. The peak to the right corresponds to atoms which were reflected by the evanescent wave. The reflected and transmitted peaks are clearly separated with a low count rate in between.

The position of the reflected peaks was approximately equal to the position expected for specular reflection (in-
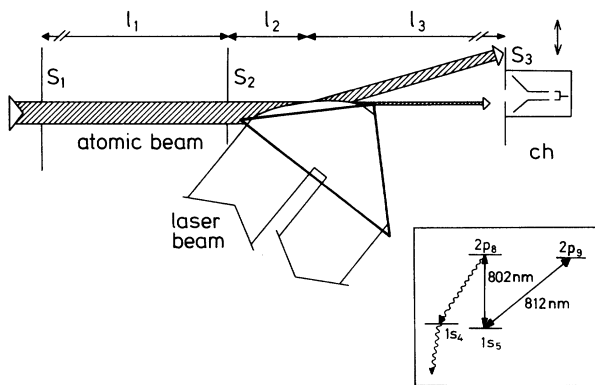

FIG. 2. Schematic diagram showing the experimental setup used for reflection of a metastable argon beam from an evanescent light field. A metastable argon beam (shown shaded) was collimated by two slits, S_1 (100 μm) and S_2 (10 μm) separated by l_1 =0.95 m. A part of the atomic beam was reflected by an evanescent light field produced at the surface of a glass prism (shown by the thicker line), l_2 =0.07 m downstream of the second slit. The far-field atomic distribution was detected by a channeltron (ch) detector (l_3 =0.58 m), which could be translated laterally. The relevant energy levels of argon are shown inset.

dicated by the dashed line in Fig. 3). As discussed above (Sec. II), near-specular reflection would be expected, because the effective Rabi frequency Ω was much larger than the spontaneous decay rate Γ and the laser beam waist was much larger than evanescent-wave decay length. Due to the finite size of the laser beam, the evanescent wave behaved as a diverging lens. Assuming normal incidence the focal lengths in the x-z and y-z planes (2.7) were $f_x \sim 50$ m and $f_y \sim 0.07$ m, respectively. The detector slit was sufficiently long (~ 2 cm) that the defocusing in the y direction did not lead to any loss of signal. In the x direction, the lens effect is expected to lead to a maximum additional divergence for the reflected atomic beam of ~ 0.3 mrad. For glancing angle incidence, the defocusing effect should be smaller, however, astigmatic aberrations become significant and the exact broadening effect of the Gaussian laser profile must be determined by a Monte Carlo simulation of the reflection process (see Sec. IV C).

The intensity of the reflected beam as a function of the incidence angle is influenced by two mechanisms: the loss of atoms which go too close to the surface and a geometrical factor arising from the overlap of the atomic beam with the evanescent wave (see Fig. 2). For $\varphi_i < 1.5$ mrad the number of reflected atoms increases with φ_i, due to the larger overlap of the mirror with the atomic beam. For $\varphi_i > 1.5$ mrad, the number of reflected atoms decreases as the transverse kinetic energy exceeds the height of the potential barrier except within a decreasingly small area around the center of the laser beam. The maximum reflection angle was ~ 3 mrad. This is about 25% less than would be expected for the Rabi frequency used in the experiment. This deviation indicates the influence of the atom-surface interaction described in Sec. II C. When the atom-surface separation is about 30 nm the energy shift described there is around the initial kinetic energy related to the normal velocity of an atom. This cannot completely explain the discrepancy between the expected and observed maximum reflection angle. But the effect of the level shift is considerably increased by the roughness of the prism surface due to the nonlinear dependence on the atom-surface separation. This may explain the discrepancy observed here and a similar loss of atoms at large deflection angles as has been observed in previous work [5,6,8].

B. Reflection by a surface-plasmon-enhanced evanescent wave

The atomic distribution produced by reflection from a surface-plasmon-enhanced evanescent wave is shown in Fig. 4. The enhancement of the evanescent wave allowed
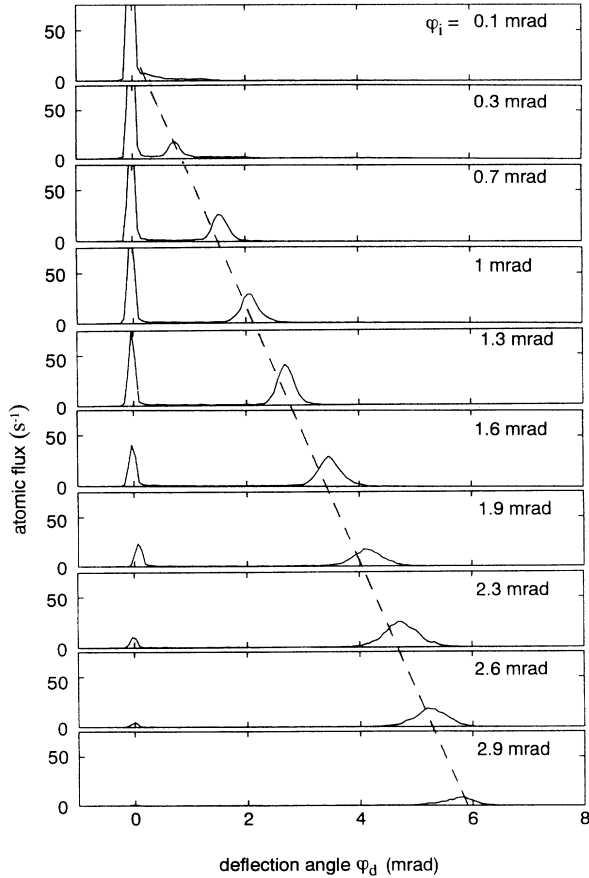

FIG. 3. Atomic intensity distribution produced by reflection of a metastable argon beam from a near-resonant evanescent wave created by total internal reflection. A sequence of results for increasing atomic beam incidence angle φ_i are shown. The dashed line indicates the angle corresponding to specular reflection ($\varphi_d = 2\varphi_i$). For experimental details see text.
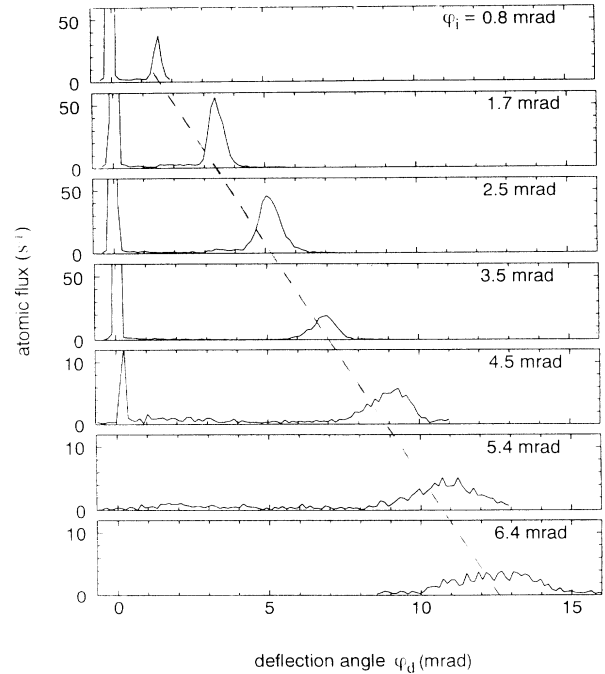

FIG. 4. Atomic intensity distribution produced by reflection of a metastable argon beam from a near-resonant evanescent wave created by surface-plasmon excitation. A sequence of results for increasing atomic beam incidence angle φ_i are shown. The dashed line indicates the angle corresponding to specular reflection ($\varphi_d = 2\varphi_i$). For $\varphi_i \geq 4.5$ mrad the vertical scale is magnified by a factor of 5. For experimental details see text.

the maximum reflection angle to be increased to 6.4 mrad (a factor of 2 larger than for the normal evanescent wave). This angle corresponds to a normal velocity of 3.6 ms^{-1}. The intensity enhancement of the surface plasmon was not measured directly but the reflection experiments indicate a value of 20±5.

Although surface plasmons offer significant field enhancement, there are possible drawbacks. The characteristic decay length of the evanescent field is determined by the dielectric constant of the metal and cannot be chosen to create a steep potential which reduces the amount of spontaneous emission. The energy of the plasmon is dissipated as heat (internal damping) in the metal film or by scattered light (radiation damping). The internal damping causes heating which can damage the film and therefore limits the maximum intensity of the evanescent wave. For an atom mirror stray light is undesirable because it can result in diffusive scattering of the atomic beam. However, for well-fabricated films, the effects of stray light should be small because the surface plasmon radiates exclusively back into the dielectric. An additional effect is that the coupling depends on the thickness of the metal layer. For an imperfect metal film this leads to significant intensity variations along the evanescent field.

Comparison of the results for the normal, Fig. 3, and surface-plasmon-enhanced evanescent waves, Fig. 4, indicates the importance of the broadening effects associated with the surface plasmon. For the same angle of incidence, the widths of the surface-plasmon-reflected peaks were approximately 20% larger. This difference can be explained by the longer decay length of the surface-plasmon field. Allowing for this effect, the results indicate that enhancement of the evanescent field by surface plasmons does not introduce any additional broadening mechanisms in the reflection process (see also Sec. IV C). This is a promising result and suggests that evanescent waves based on surface-plasmon excitation could be useful as efficient atom mirrors.

C. Monte Carlo simulation

In this section we consider the departure from ideal reflection: The reflection process was modeled by calculating atomic trajectories through the evanescent field using a Monte Carlo simulation. We regard the atom to be well localized, because its extension if regarded as a wave packet is small compared to the characteristic length of the evanescent wave $1/\alpha$, due to the high velocity of the atom. Even at the turning point the atomic wave packet is well confined due to the steep gradient of the potential. The effects of fluctuations of the dipole force, the spontaneous force (i.e., photon recoil), and defocusing due to the Gaussian profile of the laser beam are included. By comparing the experimental results with the model predictions, the importance of these effects can be assessed. First we outline the Monte Carlo simulation.

If the Rabi frequency is much larger than the spontaneous relaxation rate Γ, an elegant approach to describe the motion of atoms in a light field is provided by

the dressed-atom model [12]. For a two-level atom, the dressed-state eigenvalues are

$$U_{n,\pm}(\mathbf{r}) = (n+1)\hbar\omega_L - \frac{1}{2}\hbar\Delta \pm \frac{1}{2}\hbar\Omega(\mathbf{r}) , \qquad (4.1)$$

where n is the number of photons in the field, x and z are the coordinates parallel and perpendicular to the surface (as in Fig. 1), and the spatial dependence of the Rabi frequency is given by (2.4). The z dependence of the energy levels is depicted schematically in Fig. 5(a).

For positive detuning, an initial state consisting of an atom in the ground state and $n+1$ photons in the field evolves adiabatically into the dressed state $|+,n\rangle$. The atom climbs the potential hill and decelerates [see
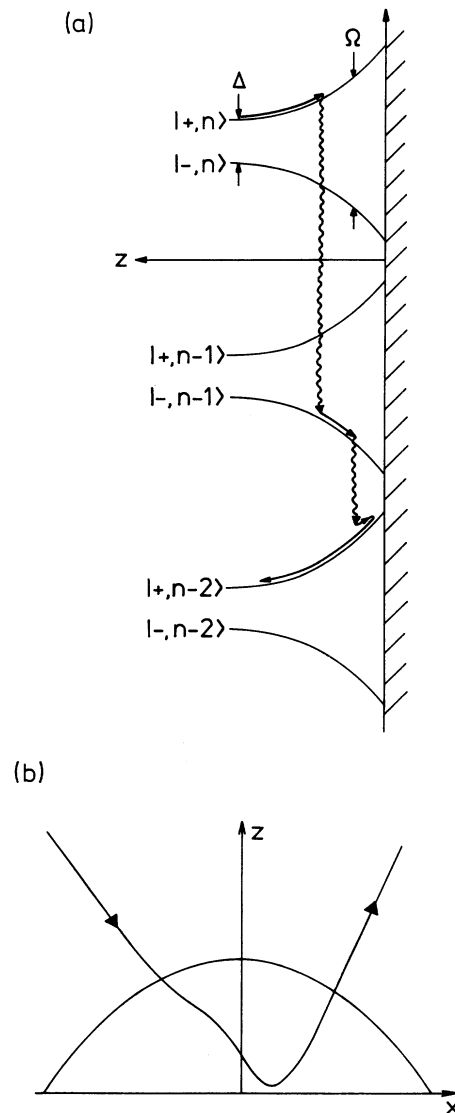

FIG. 5. Dressed-state model of the reflection process. (a) The dressed-state energy levels as a function of distance z from the surface. Spontaneous emission is described by transitions between the dressed states. The arrows show a possible history of a reflected atom. (b) Schematic depiction of the atomic trajectory corresponding to the history shown in (a).

Fig. 5(a)]. Eventually it stops and the direction of motion is reversed. As the atom moves deeper into the evanescent field, the excited state component in $\mid +,n\rangle$ and hence the probability for spontaneous emission increases. If a spontaneous emission occurs, the atom suffers a recoil and the system ends up in eigenstate $\mid +,n-1\rangle$ or $\mid -,n-1\rangle$. The net recoil is equal to the difference between the momentum of the absorbed photon (directed parallel to the surface) and the emitted photon with a random direction.

For $\Omega \gg \Gamma$, the coherence between the dressed states may be neglected (secular approximation) [12], i.e., the atom is always in one dressed state or another. If the atom lands in $\mid +,n-1\rangle$, it is affected by the same potential as before and the only change is the effect of the recoil. If it ends up in $\mid -,n-1\rangle$, it suddenly experiences an attractive potential. Even if the atom quickly decays back to a state which is affected by a repulsive potential, i.e., $\mid +,n-2\rangle$, there is a dramatic deflection of the trajectory of the atom. This deflection is depicted schematically in Fig. 5(b), which shows the atomic trajectory corresponding to history shown in Fig. 5(a).

If an atom occupies an attractive level as it approaches the surface, it tends to be deflected to a larger angle, if it occupies an attractive level while moving away, it is deflected by a smaller angle. For many atoms, the net effect is a broadening of the reflected beam.

The atomic trajectory was calculated by integrating the equation of motion

$$m\dot{\mathbf{v}} = -\nabla U_{n,\pm} , \qquad (4.2)$$

where $\mathbf{v}$ is the atomic velocity, and $U_{n,\pm}$ is the eigenvalue of the dressed state populated at time t. The van der Waals interaction of the atom with the glass prism was not taken into account here, because it depends due to its nonlinear character strongly on the surface roughness that is unknown in detail. The distribution of initial velocities was chosen to match the experimental conditions. The angular divergence of the beam was 0.1 mrad. For each time step, the probability for spontaneous emission determined by the excited state component of $\mid \pm,n\rangle$ was compared to a random variable. If spontaneous emission occurs, the potential gradient becomes that of the new dressed state and the atomic velocity is adjusted to account for recoil.

From the simulations, the relative importance of the different broadening mechanisms can be assessed. The effect of the Gaussian laser profile was determined by turning the spontaneous emission off in the simulation. The calculated divergence of the reflected beam was 0.2 mrad and 0.1 mrad for incident angles $\varphi_i = 0.8$ mrad and 6.4 mrad, respectively. These values can be compared directly with the measured divergence of the reflection beam shown in Fig. 4. For $\varphi_i > 2$ mrad, the measured divergence was much larger than defocusing effect. The additional broadening was caused by fluctuations in the dipole force induced by spontaneous emission. With spontaneous emission included there was a good agreement between the simulation and the measurements. Figure 6 shows a comparison between the calculated and
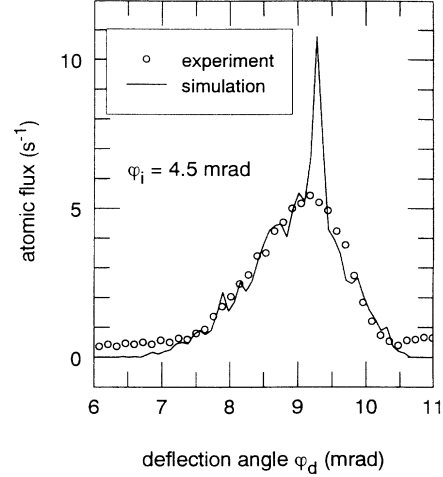
FIG. 6. Atomic intensity distribution produced by reflection of a beam of metastable argon atoms from a near-resonant evanescent wave created by surface-plasmon excitation. The angle of incidence was $\varphi_i = 4.5$ mrad. The solid curve was obtained by a Monte Carlo simulation of the reflection process.

measured atomic distribution with the surface-plasmon evanescent wave for an incident angle $\varphi_i = 4.5$ mrad. The only fit parameter was the total intensity of the calculated distribution. The narrow peak appearing in the simulation corresponds to atoms which never enter the attractive level. This peak was smeared out in the experiment due to imperfect alignment of the prism surface and the collimation slits. The width of the main distribution corresponds to a divergence of 1.2 mrad. At this incidence angle, the broadening is dominated by fluctuations in the dipole force.

A comparable agreement between the experimental results and the simulation was obtained for both normal and surface-plasmon evanescent waves for a range of incident angles. In the surface-plasmon case, the good agreement between theory and experiment implies that the surface plasmon does not introduce any additional broadening mechanism in the reflection process.

The divergence of the reflected beam is a sensitive function of the number of spontaneous emissions occurring during the reflection process. For $\varphi_i = 4.5$ mrad (Fig. 6), the average number of spontaneous emissions, determined by the simulation, was 15. For a larger reflection angle, the effective interaction time is longer and the atoms penetrate further into a region with higher Rabi frequency. Both effects lead to increased population transfer to the attractive level and a further broadening of the reflected beam. The increased broadening at large incidence angle is clearly visible in the experimental results, Figs. 3 and 4.

In addition, both in the experiment and the simulations, an asymmetry in the reflected atomic distribution was observed (see Fig. 6). This is easily explained in terms of the dressed-state picture (Fig. 5): Atoms which are deflected through a larger angle must pass closer to the surface and therefore have a greater chance of deexcitation to the electronic ground which is not detected.

Therefore the atomic intensity was lower on the larger angle side.

Finally, we emphasize that the broadening is much larger than can be accounted for by photon recoil alone. This is easily understood in terms of the dressed-state model, where spontaneous emission induces fluctuations in the sign of the force.

D. Reflection using open and closed transitions

All the results discussed so far were obtained with the "closed" transition ($1s_5 \rightarrow 2p_9$, $\lambda = 811.8$ nm). To investigate the number of spontaneous emissions, these results were compared with reflection using an "open" transition ($1s_5 \rightarrow 2p_8$, $\lambda = 801.7$ nm). The $1s_5 \rightarrow 2p_8$ transition is partially open, in that the $2p_8$ state decays either to $1s_4$ or $1s_5$ with a branching ratio of ξ:1 where $\xi = 2.4$. The $1s_4$ state decays to the electronic ground state (see inset, Fig. 2). The result is that for each spontaneous emission roughly 71% of the atoms end up in the electronic ground state and are not seen by the detector. The spontaneous lifetimes of the open and closed transitions were $\Gamma_o^{-1} = 104$ ns and $\Gamma_c^{-1} = 27$ ns. The open and closed transitions were compared using both the normal and surface-plasmon-enhanced evanescent waves.

Figure 7 shows the reflected intensity as a function of the effective detuning (defined relative to the resonance frequency of the mean velocity class) for both transitions. These results were taken with surface-plasmon-enhanced evanescent wave. The angle of incidence was $\varphi_i = 0.8$ mrad and the laser power was 1 W. The Rabi frequencies were 3.5 GHz and 1.7 GHz for the closed and open transitions, respectively. For the closed transition,
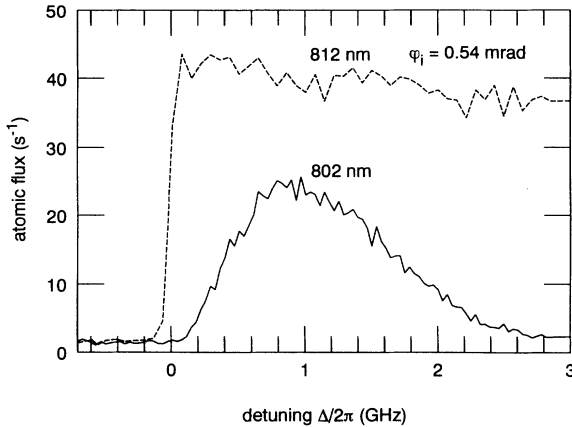

FIG. 7. Atomic intensity distribution produced by reflection of a metastable argon beam from an evanescent wave created by surface-plasmon excitation as a function of the atom-laser detuning. The dashed and solid curves correspond to evanescent waves resonant with the $1s_5 \rightarrow 2p_9$ (812 nm) and $1s_5 \rightarrow 2p_8$ (802 nm) transitions in argon. The $2p_8$ state may decay to the electronic ground state which is not detected. The ratio of the reflected intensity for the $\lambda = 812$ nm ("closed") and $\lambda = 802$ nm ("open") transition gives a measure of the number of spontaneous emissions occurring during the reflection process.

the reflected intensity increased sharply from zero for red (negative) detuning, to a roughly constant value for blue (positive) detuning. The width of the step was due to the finite velocity distribution of the atomic beam. For the open transition, the step was less pronounced due to loss of atoms which decay to the electronic ground state. The reflected atomic beam intensity reached a maximum at the relatively large detuning of 1 GHz, where spontaneous emission was less important. The reflected beam intensity was less than for the open transition due to residual decay to the undetected electronic ground state and the lower Rabi frequency. However, the relatively high reflectivity ($\sim$ 63% compared to the closed transition) indicates that stray light from the surface plasmon was not a serious problem. For large detuning, the reflected intensity for the open transition fell away faster due to the lower Rabi frequency.

By comparing the number of reflected atoms for the open and closed transitions, N_o and N_c, it is possible to place an upper bound on the probability for spontaneous emission. By assuming that the loss of atoms is completely accounted for by spontaneous emission, it follows that the number of spontaneous emissions is

$$n_{\max} = \left(1 + \frac{1}{\xi}\right) \ln\left(\frac{N_c}{N_o}\right), \qquad (4.3)$$

where ξ is the branching ratio. For the maximum value of N_o in Fig. 7, one finds $n_{\max} = 0.75$. For comparison, one can estimate the number of spontaneous emissions from the effective interaction time and the excited state intensity. For small angles, the atom does not penetrate to regions of high Rabi frequency, one may assume $\Delta \gg \omega_1$ and therefore the number of spontaneous emissions is

$$n_{\mathrm{calc}} = \frac{2\pi}{\alpha\lambda_{\mathrm{dB}}} \frac{\Gamma_o}{\Delta} \varphi_i . \qquad (4.4)$$

For the de Broglie wavelength $\lambda_{\mathrm{dB}} = 18$ pm, $\Delta = 2\pi \times 1$ GHz, $\varphi_i = 0.8$ mrad, the number of spontaneous emissions is $n_{\mathrm{calc}} = 0.28$, which is less than $n_{\max}$, as expected.

To reduce the influence of spontaneous emission, reflection under small incident angles was studied. At small incidence angles, the atoms do not penetrate deeply into the evanescent field. Therefore the maximum Rabi frequency experienced by atoms is less than the detuning. The spatial distribution of reflected atoms using both the open and closed transitions is shown in Fig. 8. These results were obtained with an evanescent wave produced by total internal reflection, the angle of incidence was $\varphi_i = 0.29$ mrad, and detunings were $\Delta = 2\pi \times 0.6$ GHz and $\Delta = 2\pi \times 0.2$ GHz for the open and closed transitions, respectively. For these parameters $n_{\mathrm{calc}} = 0.15$ and from the data one finds $n_{\max} = 0.39$. It is interesting to note that the open transition atom mirror improves the coherence of the reflected beam by selecting atoms which have not undergone spontaneous emission. If one assumes that the number of atoms making more than one spontaneous emission was negligible, the number of spontaneous emissions for atoms which were reflected and survived in the metastable state was less than $n_{\max}/(1 + \xi) = 0.11$.
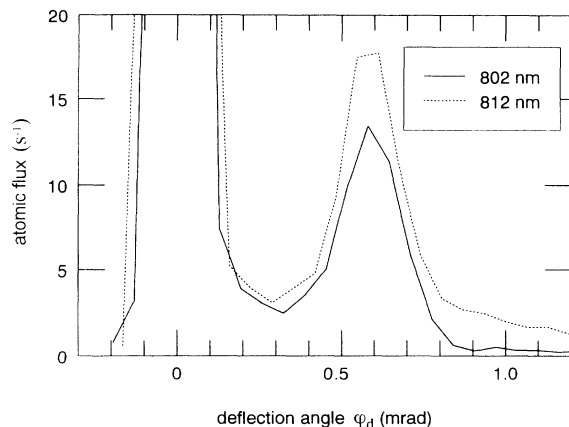
FIG. 8. Comparison of the spatial distribution of reflected atoms for the closed and open transitions. The incident angle was $\varphi_i = 0.29$ mrad and the detunings were $\Delta = 2\pi \times 0.6$ GHz and $\Delta = 2\pi \times 0.2$ GHz for the open and closed transitions, respectively. For these parameters, the average number of spontaneous emissions for reflected atoms using the open transition was less than 11%.

V. CONCLUSION

The reflection of metastable argon atoms from evanescent waves produced by total internal reflection and surface-plasmon excitation was investigated. For the surface-plasmon-enhanced evanescent wave, reflection of atoms with a normal velocity component up to 3.6 ms^{-1} was demonstrated. The departure from ideal reflection was studied in detail. We developed a Monte Carlo simulation, which provides both an intuitive and quantitative description of various mechanisms leading to additional divergence of the reflected atomic beam. There was a good agreement between the predictions of the simulation and our experimental results. Our analysis also helps to explain the broadening of the reflected beam observed in earlier work.

We showed, for small detuning and large incident angles, that the broadening of the reflected atomic beam was dominated by fluctuations of the dipole force caused by spontaneous emission. We were able to estimate the average number of spontaneous emissions by comparing reflection from evanescent waves resonant with open and closed transitions in argon. For small incident angles and a large detuning, the average number of spontaneous emissions for reflected atoms was less than 0.11. This is sufficiently small to allow the application of the mirror in an atom interferometer. For example, a Lloyd's mirror for atoms would be a useful tool to study the phase of atomic de Broglie waves interacting with a surface.

Further reduction in the destructive influence of spontaneous emission would lead to the attractive goal of near-perfect coherent reflection. This could be achieved using larger laser detunings, in which case a large enhancement of the evanescent wave is important to maintain the height of the optical potential. Here we showed that surface plasmons produce a significant enhancement without degrading the quality of reflection. The amount of spontaneous emission may be reduced by using evanescent fields with a steeper exponential decay. A particularly promising technique is the dielectric waveguide [10,11] which combines large enhancement and a steep potential.

Atom mirrors are an important component for future progress in the field of atom optics. Curved evanescent-wave mirrors may be employed to focus atoms. Such a curved mirror is the main component in a gravito-optical cavity [20]. Atom cavities could be used to accumulate a dense cloud of cold atoms and is a promising candidate for the observation of quantum statistical effects.

[1] O. Stern, Naturwissenschaften **17**, 391 (1929); F. Knauer and O. Stern, Z. Phys. **53**, 779 (1929); I. Estermann and O. Stern, *ibid.* **61**, 95 (1930).

[2] *Optics and Interferometry with Atoms*, edited by J. Mlynek, V. I. Balykin, and P. Meystre, special issue of Appl. Phys. B **54** (1992); M. Sigel, C. S. Adams, and J. Mlynek, in *Frontiers in Laser Spectroscopy*, Proceedings of the International School of Physics "Enrico Fermi," Course CXX, edited by T. W. Hänsch and M. Inguscio (North-Holland, Amsterdam, in press).

[3] See, for example, K. H. Rieder, Contemp. Phys. **26**, 559 (1985).

[4] R. J. Cook and R. K. Hill, Opt. Commun. **43**, 258 (1982).

[5] V. I. Balykin, V. S. Letokhov, Yu. B. Ovchinnikov, and A. I. Sidorov, Pis'ma Zh. Eksp. Teor. Fiz. **45**, 282 (1987) [JETP Lett. **45**, 353 (1987)].

[6] M. Kasevich, D. Weiss, and S. Chu, Opt. Lett. **15**, 607 (1990).

[7] C. G. Aminoff, A. M. Steane, P. Bouyer, P. Desbiolles, J. Dalibard, and C. Cohen-Tannoudji, Phys. Rev. Lett. **71**, 3083 (1993).

[8] T. Esslinger, M. Weidemüller, A. Hemmerich, and T. Hänsch, Opt. Lett. **18**, 450 (1993).

[9] S. Feron, J. Reinhardt, S. Le Boiteux, O. Gorceix, J. Baudon, M. Ducloy, J. Robert, Ch. Miniatura, S. Nic Chormaic, H. Haberland, and V. Lorent, Opt. Commun. **102**, 83 (1993).

[10] R. Kaiser, Y. Lévy, N. Vansteenkiste, A. Aspect, W. Seifert, D. Leipold, and J. Mlynek, Opt. Commun. **104**, 234 (1994).

[11] W. Seifert, R. Kaiser, A. Aspect, and J. Mlynek (unpublished).

[12] J. Dalibard and C. Cohen-Tannoudji, J. Opt. Soc. Am. B **2**, 1707 (1985).

[13] C. Cohen-Tannoudji, in *Atomic Motion in Laser Light* in *Fundamental Systems in Quantum Optics*, edited by J. Dalibard, J.-M. Raimond, and J. Zinn-Justin (North-Holland, Amsterdam, 1992).

[14] M. Born and E. Wolf, *Principles of Optics* (Pergamon Press, Oxford, 1970).

[15] H. Raether, *Surface Plasmons* (Springer, Berlin, 1988).

[16] *CRC Handbook of Chemistry and Physics*, 68th ed., edited by R. C. Weast (CRC Press, Boca Raton, 1988).

[17] P. B. Johnson and R. W. Christy, Phys. Rev. B **6**, 4370 (1972).

[18] D. Meschede, W. Jhe, and E. A. Hinds, Phys. Rev. A **41**, 1587 (1990).

[19] H. Conrad, G. Ertl, J. Küppers, W. Sesselmann, B. Woratschek, and H. Haberland, Surf. Sci. **117**, 98 (1982).

[20] H. Wallis, J. Dalibard, and C. Cohen-Tannoudji, Appl. Phys. B **54**, 407 (1992).